

Supplementary Materials for

A neuronal molecular switch through cell-cell contact that regulates quiescent neural stem cells

Jian Dong, Yuan-Bo Pan, Xin-Rong Wu, Li-Na He, Xian-Dong Liu, Dong-Fu Feng, Tian-Le Xu, Suyu Sun*, Nan-Jie Xu*

*Corresponding author. Email: xunanjie@sjtu.edu.cn (N.-J.X.); sunsuya@shsmu.edu.cn (S.S.)

Published 27 February 2019, *Sci. Adv.* **5**, eaav4416 (2019)

DOI: 10.1126/sciadv.aav4416

The PDF file includes:

- Fig. S1. Activated GC neurons after treatment of contextual fear, enriched environment exposure, or voluntary running, respectively.
 - Fig. S2. Unchanged total GFP⁺ NSCs and increased Ki67⁺ rNSCs and ANPs after running.
 - Fig. S3. Increased DCX⁺ cells and Tbr2⁺ cells in the hippocampus after voluntary running.
 - Fig. S4. Excited DG glutamatergic neurons but not GABAergic neurons in voluntary running.
 - Fig. S5. AAV-infected vGluT2⁺-specific DG neurons.
 - Fig. S6. c-Fos⁺ neurons in the DG region after CNO treatment in various doses.
 - Fig. S7. Effects of CNO control with various doses.
 - Fig. S8. Analysis of sequencing results.
 - Fig. S9. Ephrin-B3 ligand prevents proliferation/differentiation of aNSCs and their transition to neurons.
 - Fig. S10. EphB2 kinase-dependent signaling is required for the maintenance of quiescent rNSCs.
- Legends for movies S1 to S3

Other Supplementary Material for this manuscript includes the following:

(available at advances.sciencemag.org/cgi/content/full/5/2/eaav4416/DC1)

- Movie S1 (.mp4 format). Voluntary running behavior of a mouse in the running wheel.
- Movie S2 (.mp4 format). In vivo fiber photometry of Ca²⁺ signal of DG granule neurons during running trials.
- Movie S3 (.mp4 format). 3D reconstruction of confocal images of rNSCs and GCs.

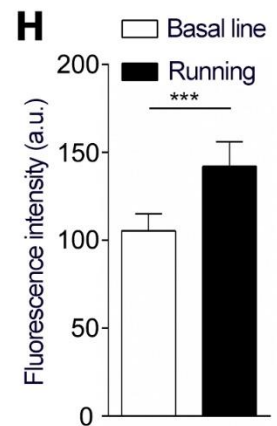
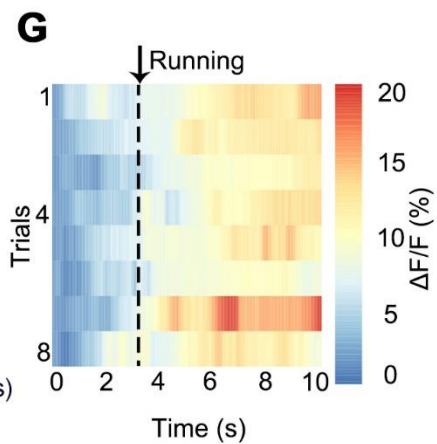
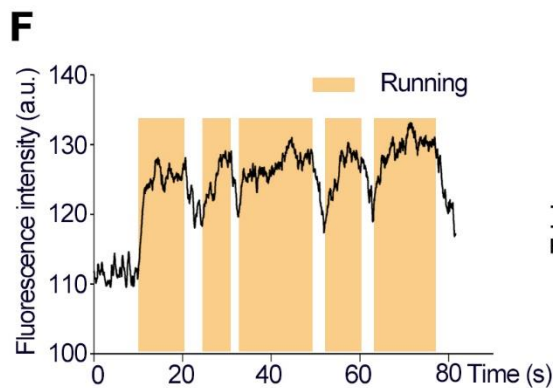
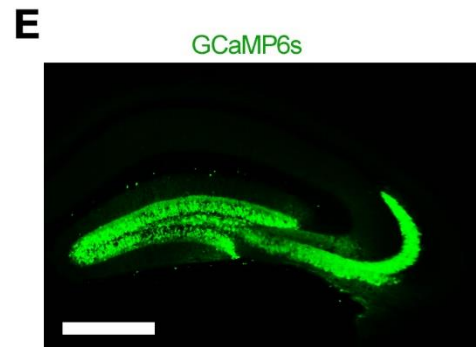
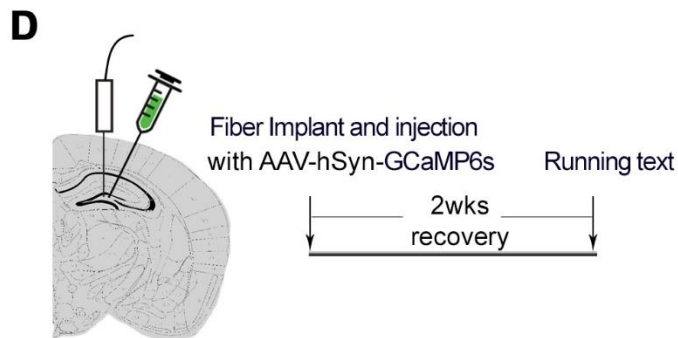
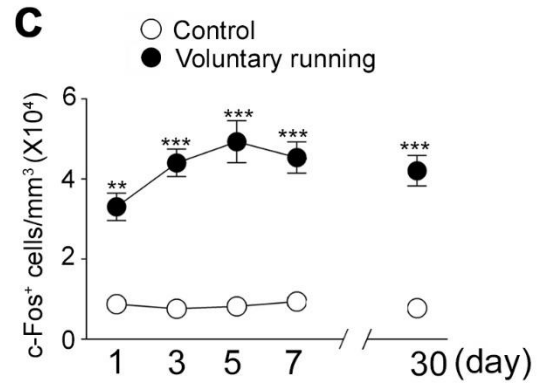
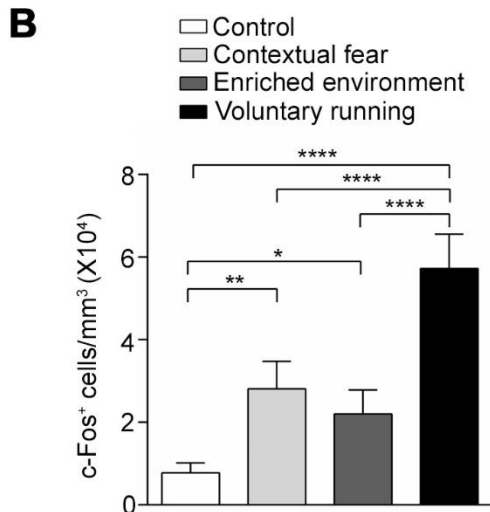
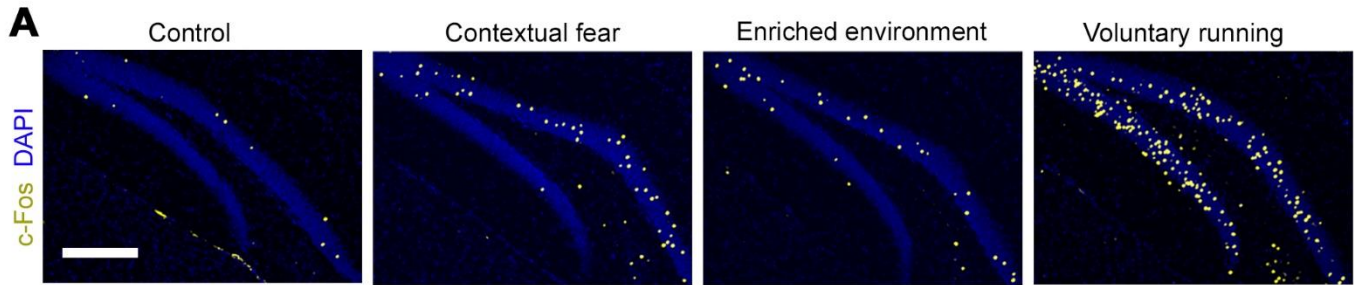


Fig. S1. Activated GC neurons after treatment of contextual fear, enriched environment exposure, or voluntary running, respectively. (A) Representative images of c-Fos⁺ cells in DG region of control, contextual fear, enriched environment exposure, or voluntary running. Scale bar, 200 μ m. (B) Quantification of the density of c-Fos⁺ cells in control, contextual fear, enriched environment exposure, or voluntary running. n = 4 for control, and n = 4 for Running group. (C) Quantification of the density of c-Fos⁺ cells in control and running mice after treating 1, 3, 5, 7 or 30 days. n = 4 mice. (D) AAV2/9-hSyn-GCaMP6s injected and optic fiber implanted scheme to the DG for in vivo Ca²⁺ fiber photometry experiment. (E) Composite images showing infected GFP⁺ cells in DG regions. Scale bar, 500 μ m. (F) Representative trace of fluorescence density from infected granule cell population representing the Ca²⁺ signal *in vivo*. Time course of GCaMP6s fluorescence transient event-locked to running. (G) Representative heat map of $\Delta F/F$ changes of 8 trials from mice. We derived the values of fluorescence change ($\Delta F/F$) by calculating $(F-F_0)/F_0$, where F_0 is the baseline fluorescence signal averaged over a 2-s-long time window. (H) Quantification of the intensity of GCaMP6s fluorescence of basal level and during running trails. n = 8 mice. Result presented as mean \pm SEM. * P < 0.05; ** P < 0.01; *** P < 0.001; **** P < 0.0001.

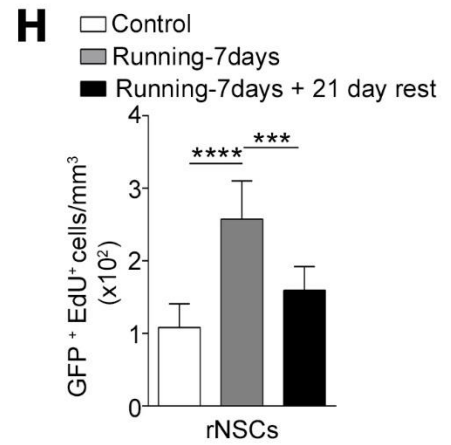
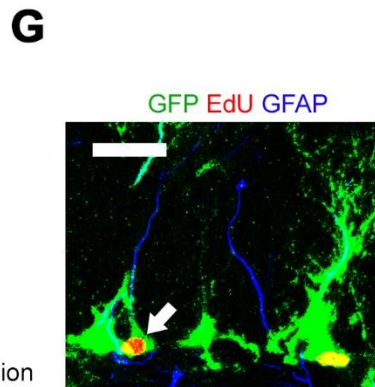
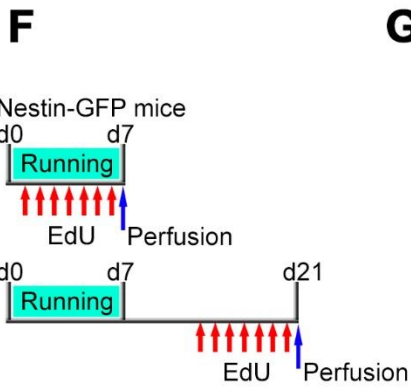
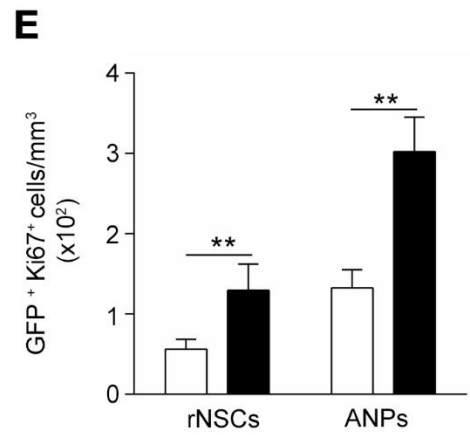
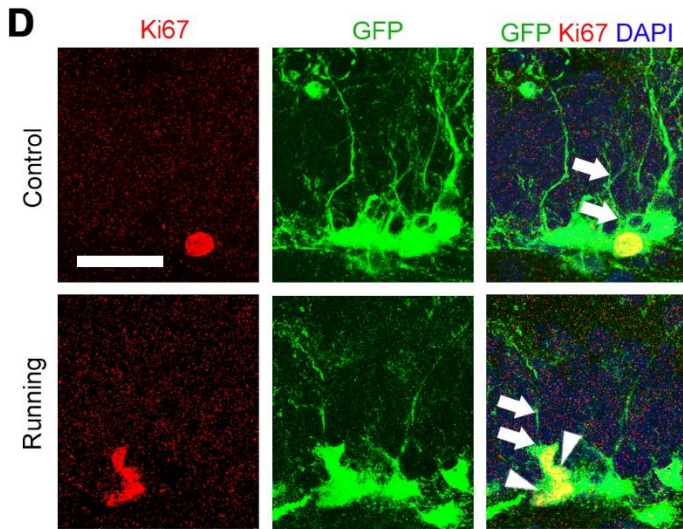
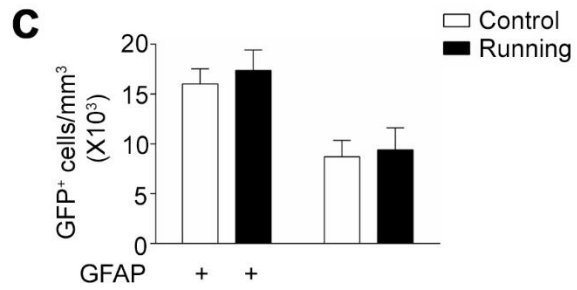
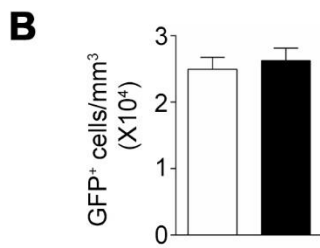
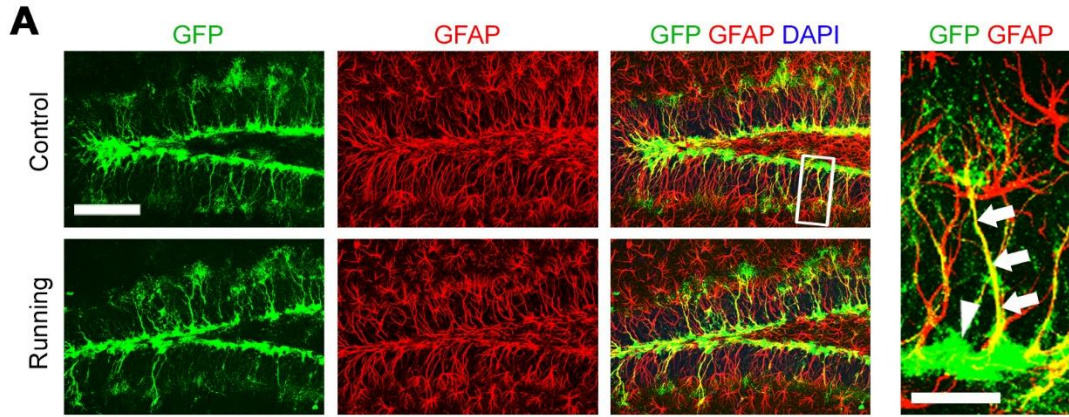


Fig. S2. Unchanged total GFP⁺ NSCs and increased Ki67⁺ rNSCs and ANPs after running. (A) Composite confocal images showing total GFP⁺ cells and image immunostaining with GFAP to distinguish rNSCs (arrows) and ANPs (arrowheads) of control and running mice. Scale bar, 100 μ m (left) and 50 μ m (right zoomed in). (B) Quantification of total of GFP⁺ cells in control and running mice after treating. n = 4 for control group, and n = 4 for running group. (C) Quantification of number of rNSCs and ANPs in control and running mice after treating. n = 4 for control group, and n = 4 for running group. (D) Composite confocal images of the GFP⁺ cells immunostaining with Ki67 in the DG from control and running groups. Scale bar, 50 μ m. (E) Quantification of the density of Ki67⁺ rNSC and ANP in control and running mice. (n = 4 for each group). (F) The established protocol used for voluntary running induced hippocampal rNSCs activation and neurogenesis. Ten-week-old mice had access to a running wheel for 7-day running and a group of mice treated with 7-day running followed by 21-day rest and EdU injection (once per day for 7-day) before brain sectioning for immunostaining. (G) Composite confocal images showing EdU incorporation cells of rNSCs (arrows). Scale bar, 25 μ m. (H) Density of EdU incorporation cells of rNSC. n = 4 mice for each group. Result presented as mean \pm SEM. ** P < 0.01 *** P < 0.001; **** P < 0.0001.

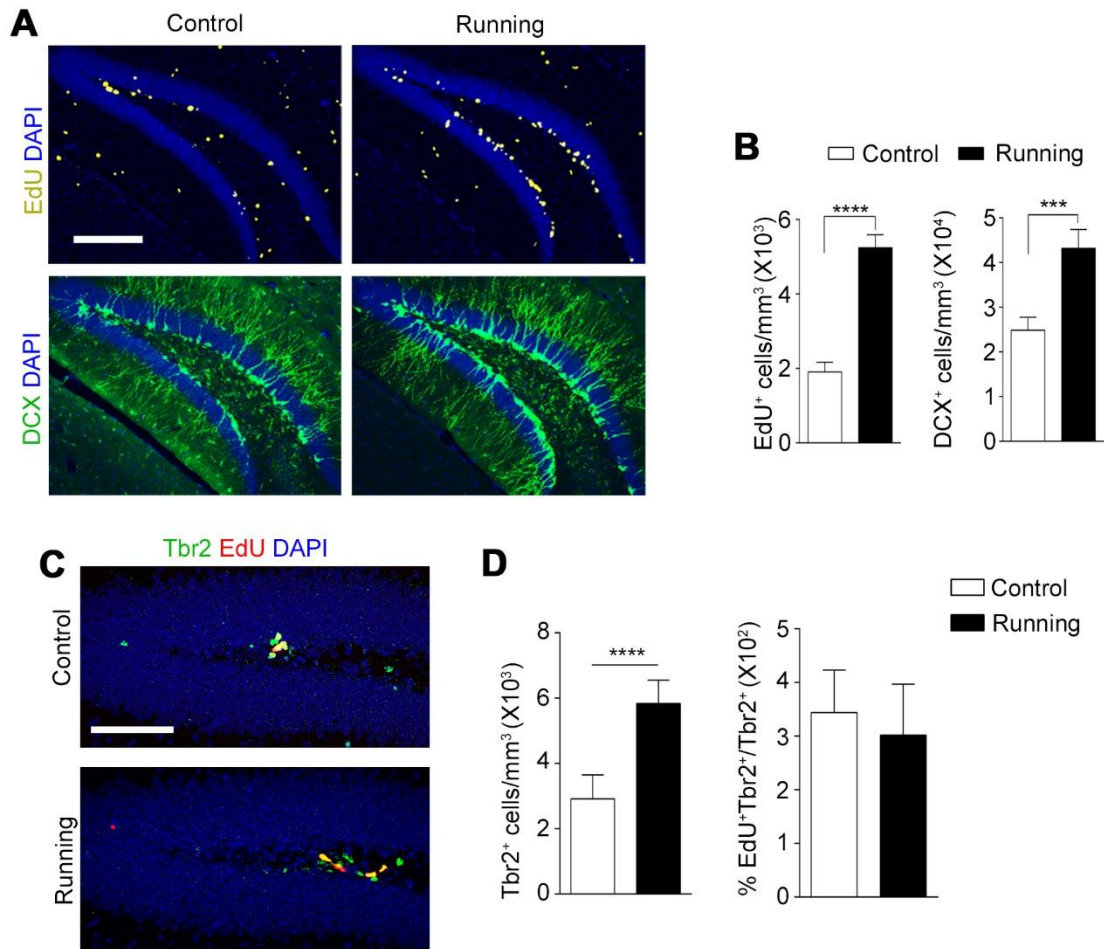


Fig. S3. Increased DCX⁺ cells and Tbr2⁺ cells in the hippocampus after voluntary running. (A) Images of the EdU⁺ and DCX⁺ cells in the DG from control and running groups. Scale bar, 200 μ m. (B) Quantification of the density of EdU⁺ and DCX⁺ cells in control and running mice. n = 4 for control group, and n = 4 for running group. (C) Confocal images of the Tbr⁺ cells in the DG from control and running groups. Scale bar, 100 μ m. (D) Quantification of the density of Tbr2⁺ cells in control and running mice. n = 6 for control group, and n = 7 for running group. Result presented as mean \pm SEM. *** P < 0.001; **** P < 0.0001.

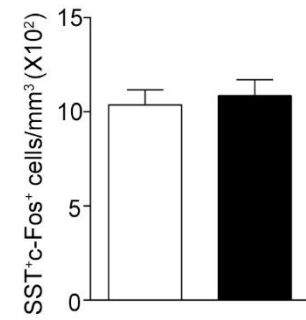
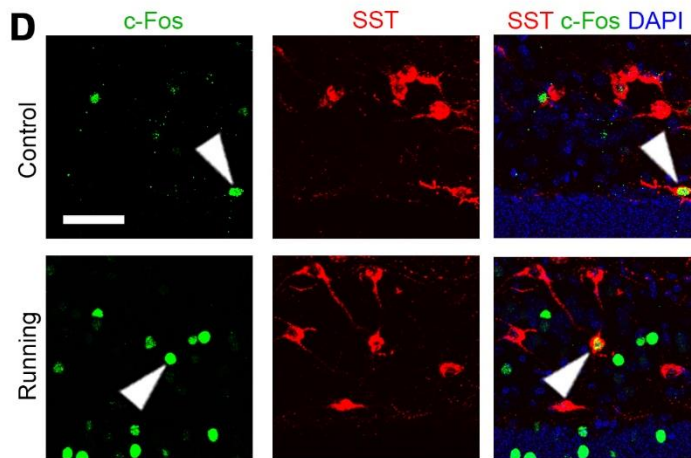
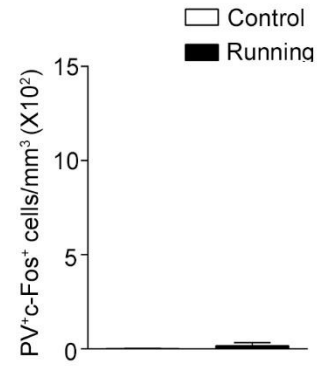
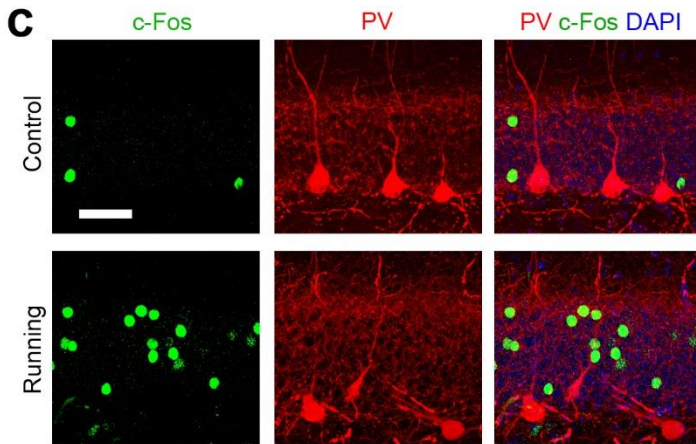
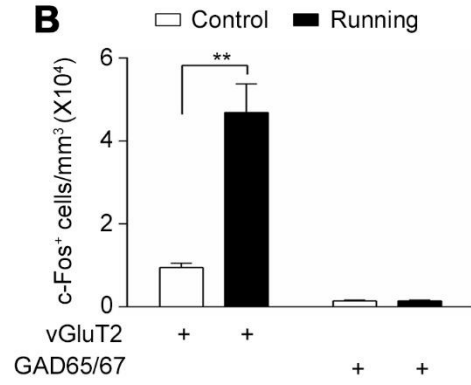
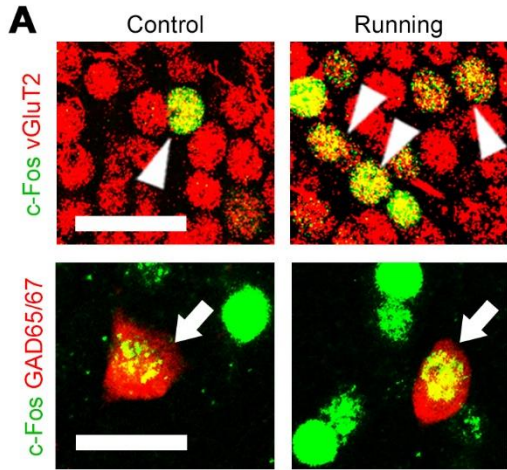


Fig. S4. Excited DG glutamatergic neurons but not GABAergic neurons in voluntary running. (A) Merged confocal images showing c-Fos⁺ cells immunostaining with vGluT2 or GAD65/67 after voluntary running. Scale bar, 25 μ m. (B) Quantification of the density of c-Fos⁺ vGluT2⁺ cells and c-Fos⁺ GAD65/67⁺ respectively in control and voluntary running mice. n = 4 for control group, and n = 4 for running group. (C) Composite confocal images showing c-Fos⁺ cells immunostaining with PV⁺ neurons after voluntary running. Scale bar, 50 μ m. (D) Composite confocal images showing c-Fos⁺ cells immunostaining with SST⁺ neurons after voluntary running. Scale bar, 50 μ m. Result presented as mean \pm SEM. ** P < 0.01.

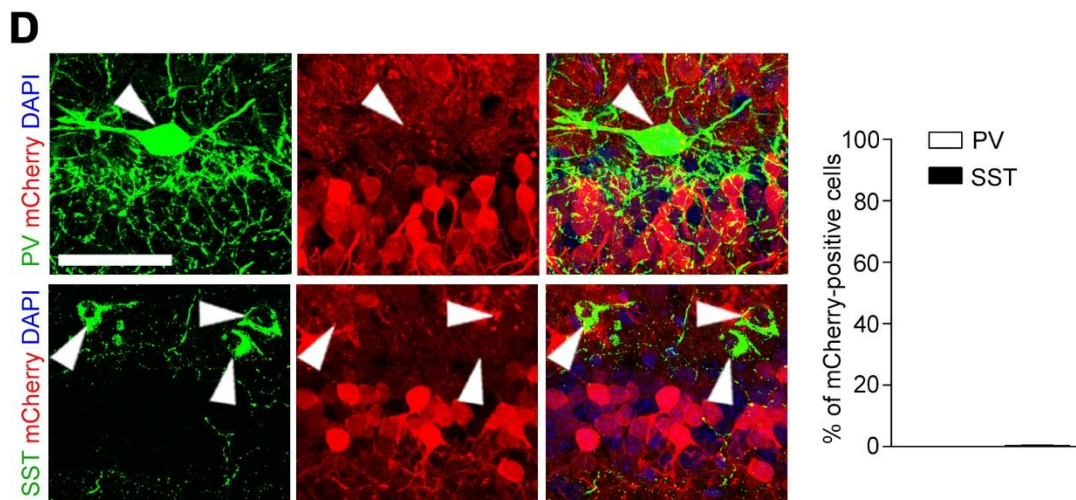
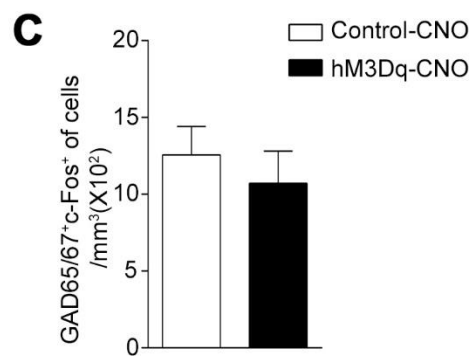
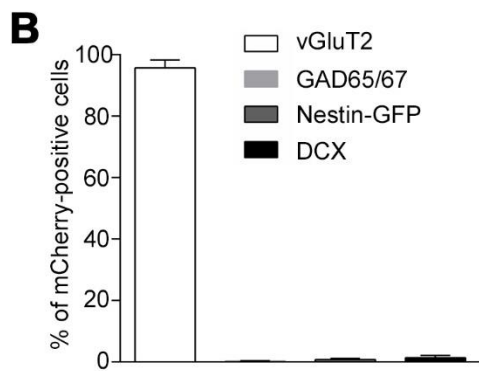
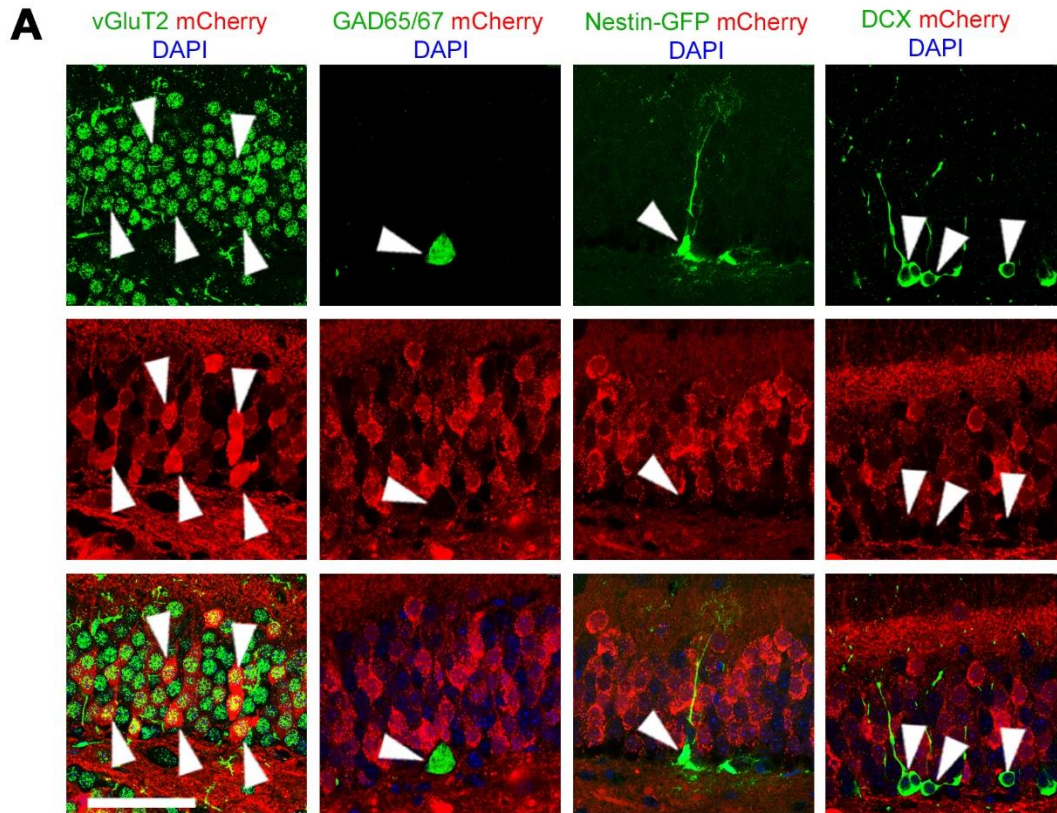


Fig. S5. AAV-infected vGluT2⁺-specific DG neurons. (A) Composite confocal images showing mCherry⁺ cells immunostaining with vGluT2, GAD65/67, GFP, and DCX after AAV injection. Scale bar, 60 μ m. (B) Quantification of the density of mCherry⁺ vGluT2⁺ cells, mCherry⁺ GAD65/67⁺ cells, mCherry⁺ GFP⁺ cells and mCherry⁺ DCX⁺ cells (4013 vGluT2⁺, 19 GAD65/67⁺, 26 Nestin-GFP⁺, 13 DCX⁺ cells from 4 mice were counted). n = 4 for each group. (C) Quantification of the density of GAD65/67⁺ c-Fos⁺ cells in control and chemogenetic excitation group. n = 4 for each group. (D) Composite confocal images and quantification of the density of mCherry⁺ cells immunostaining with PV and SST after AAV injection (0 PV⁺ and 2 SST⁺ cells of 4878 mCherry⁺ cells from 4 mice were counted). Scale bar, 50 μ m. Result presented as mean \pm SEM.

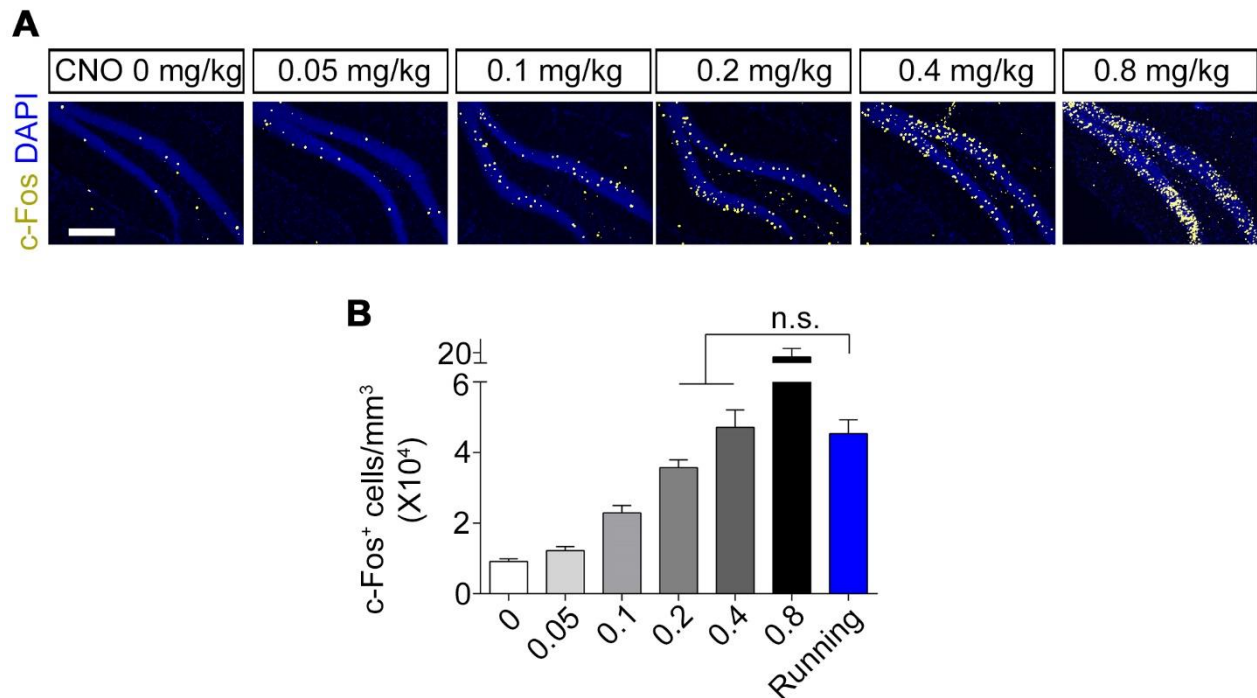


Fig. S6. c-Fos⁺ neurons in the DG region after CNO treatment in various doses. (A) Composite images showing c-Fos⁺ neurons after CNO treatment in doses range of 0.05-0.8 mg/kg i.p. in hM3Dq infected mice. Scale bar, 200 μ m. (B) Quantification of the density of c-Fos⁺ neurons after CNO treatment. n = 4 for each group. Result presented as mean \pm SEM.

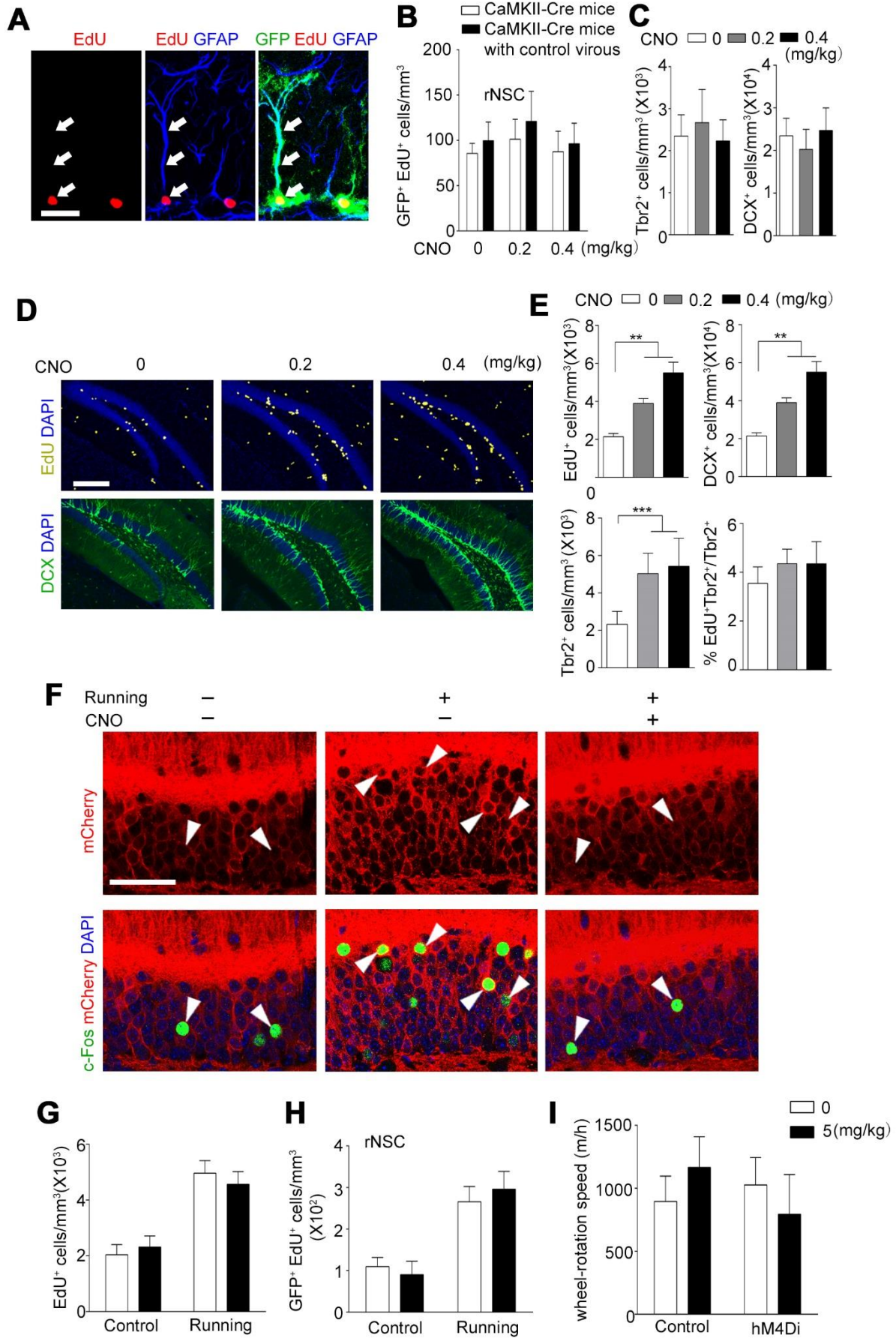
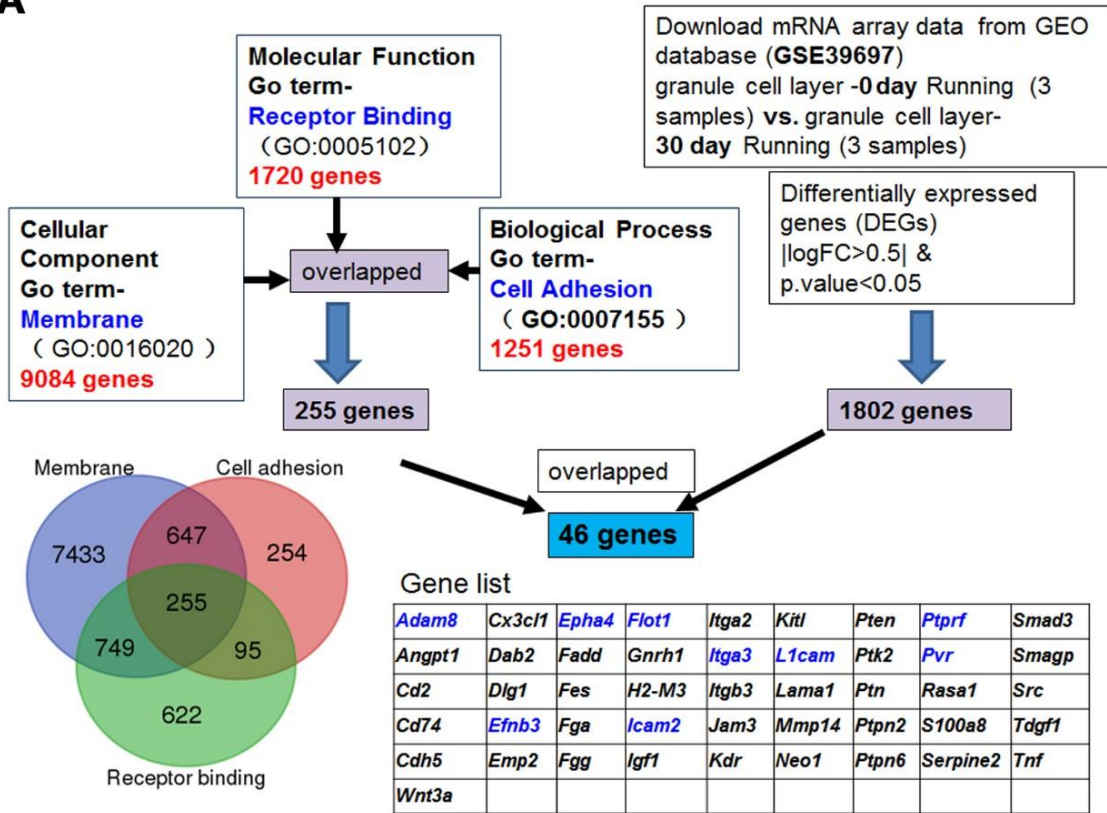


Fig. S7. Effects of CNO control with various doses. (A) Composite confocal images showing EdU incorporated rNSCs (arrows). Scale bar, 50 μm . (B) Density of EdU incorporated rNSCs in the DG after CNO treatment in the concentration of 0, 0.2 and 0.4 mg/kg in CaMKII-Cre mice with/without control virus injection. n = 4 for each group. (C) Quantification for density of DCX⁺ and Tbr2⁺ cells in the DG after CNO treatment in the concentration of 0, 0.2 and 0.4 mg/kg in control virus injected CaMKII-Cre mice. n = 4 for each group. (D) Images of the EdU⁺ and DCX⁺ cells in the DG after CNO treatment in the concentration of 0, 0.2 and 0.4 mg/kg. Scale bar, 200 μm . (E) Quantification of the density of EdU⁺, DCX⁺, Tbr2⁺ and EdU⁺ Tbr2⁺ cells in the DG after CNO treatment in the concentration of 0, 0.2 and 0.4 mg/kg. n = 5 for each group. (F) Confocal images of c-Fos⁺ cells in DG of following chemogenetic inhibition by AAV-DIO-hM4Di-mCherry virus injection in CaMKII-Cre; Nestin-GFP mice under voluntary running trials. Scale bar, 50 μm . (G) Quantification of the density of EdU⁺ cells in the DG after CNO treatment in the concentration of 0, 5 mg/kg in control virus groups after running treatment. n = 6 for each group. (H) Quantification of the density of EdU⁺ rNSCs cells in the DG after CNO treatment in the concentration of 0, 5 mg/kg in control virus groups after running treatment. n = 6 for each group. (I) Quantification of the daily running distance after CNO treatment in the concentration of 0, 5 mg/kg after running treatment. n = 6 for each group. Result presented as mean \pm SEM. ** P < 0.01; *** P < 0.001.

A



B

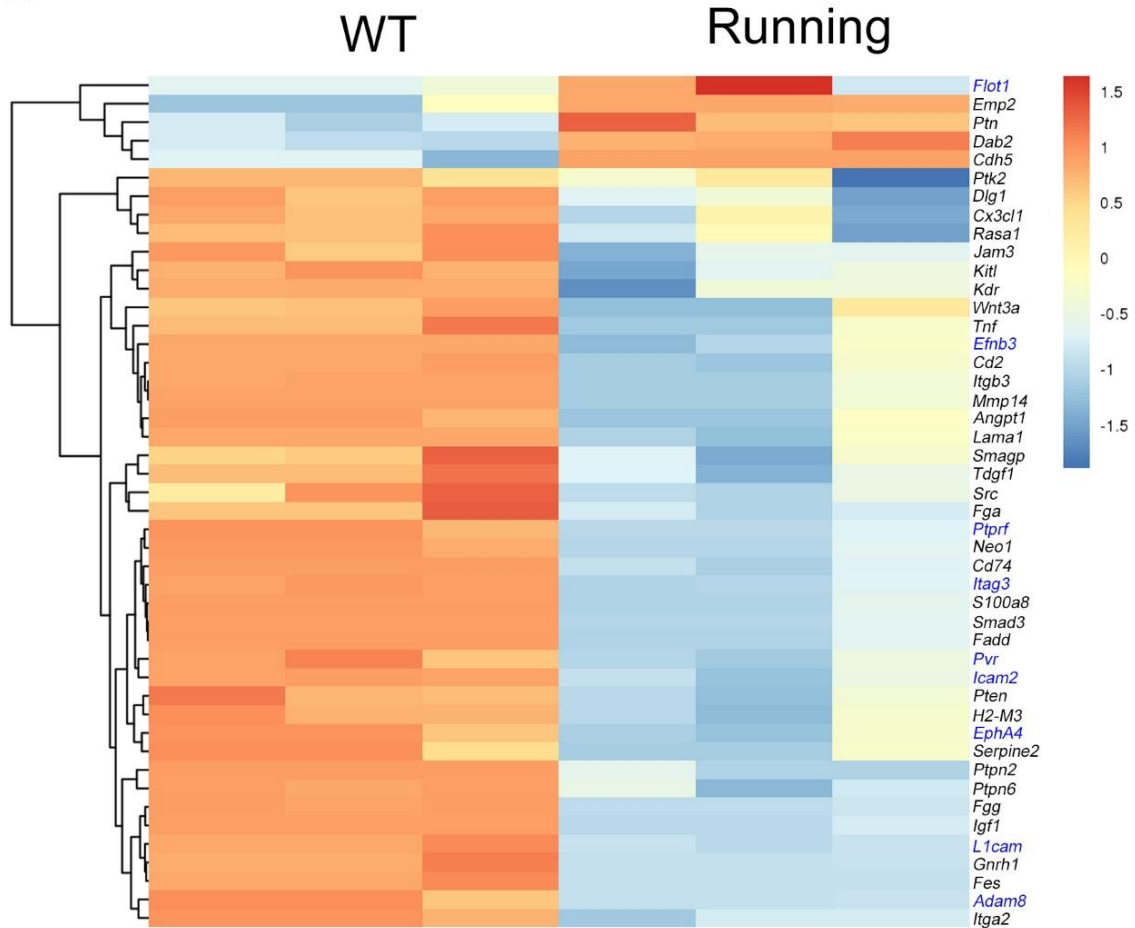


Fig. S8. Analysis of sequencing results. (A) The established protocol used for analyzing of running sequencing result. Sequencing results reported previously (Miller et al., 2013) was analyzed. The genes that were changed after running treatment over 30 days were significantly enriched in GO terms of cell adhesion, receptor binding, and membrane. Total 255 common genes were obtained by merging the three GO terms, and were further compared with 1802 differentially expressed genes (DEGs) in granule cell layer of DG after running treatment to obtain 46 overlapped genes. (B) Heat map of 46 Genes with differential expression. Result presented as mean \pm SEM.

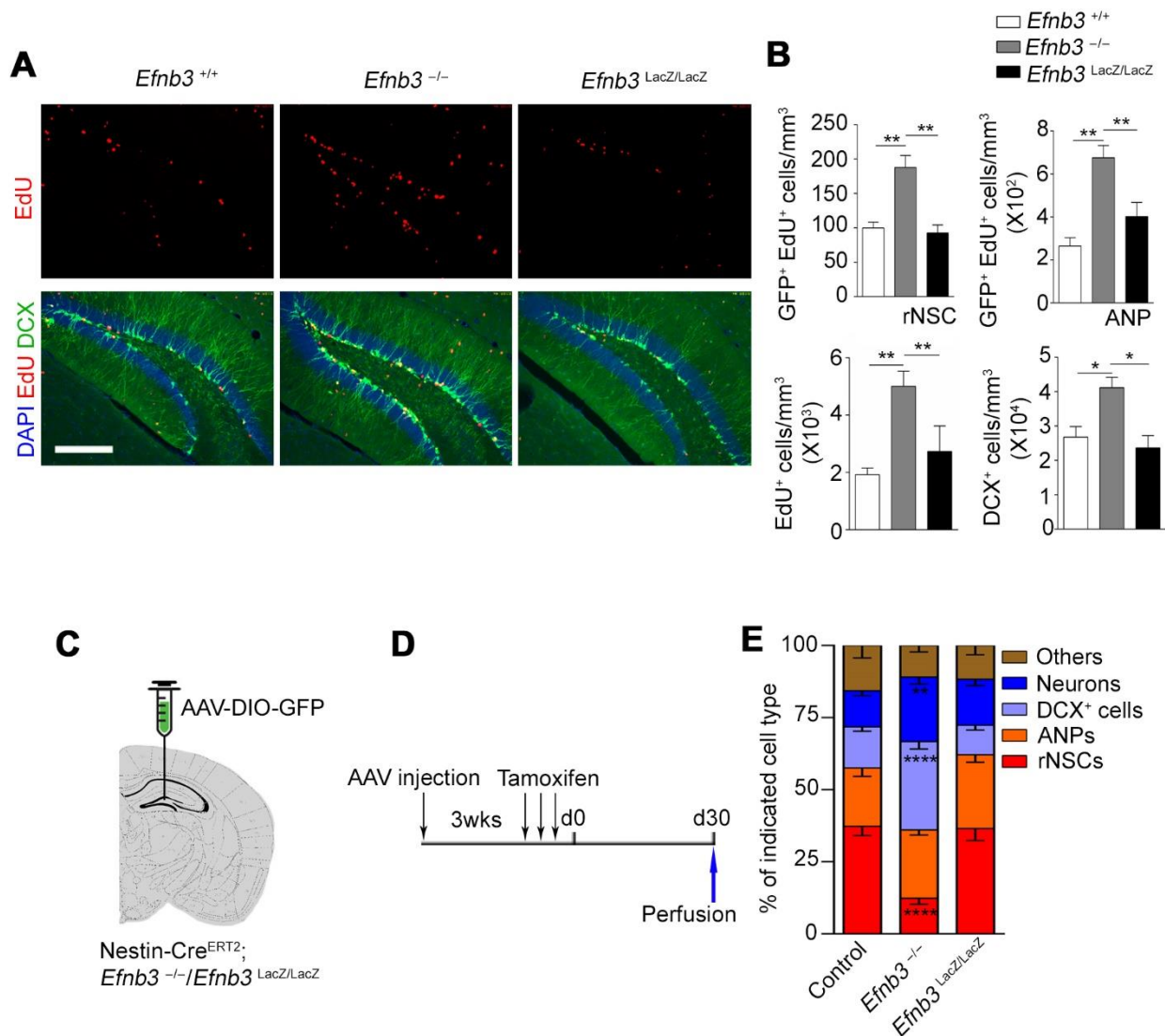


Fig. S9. Ephrin-B3 ligand prevents proliferation/differentiation of aNSCs and their transition to neurons. (A) Images of EdU⁺ and DCX⁺ adult NSCs in $Efnb3^{+/+}$, $Efnb3^{-/-}$ and $Efnb3^{LacZ/LacZ}$ mice. Scale bar represents 50 μ m. (B) Quantitative analysis showing that $Efnb3^{-/-}$ mice have increased numbers in either EdU⁺ rNSCs/ANPs or DCX⁺ cells compared with control mice, while the $Efnb3^{LacZ/LacZ}$ mice remain unchanged. n = 4 for each group. (C) AAV-DIO-GFP injection scheme to the DG of Nestin-Cre^{ERT2}; $Efnb3^{-/-}$ mice/ $Efnb3^{LacZ/LacZ}$ mice. (D) Scheme depicting experimental procedure of lineage tracing pertaining to injection of viruses into the DG of Nestin-Cre^{ERT2}; $Efnb3^{-/-}$ mice/ $Efnb3^{LacZ/LacZ}$ mice. (E) Graph shows the proportion of the different cell types in the niche quantified of all GFP⁺ cells of Nestin-Cre^{ERT2} mice. Control group: 3024 GFP⁺ cells of 38 brain slices were counted; n = 5 mice; $Efnb3^{-/-}$ group: 3689 GFP⁺ cells of 43 brain slices were counted; n = 7 mice; $Efnb3^{LacZ/LacZ}$ group: 3214 GFP⁺ cells of 42 brain slices were counted; n = 6 mice. Result presented as mean \pm SEM. **P < 0.01; ***P < 0.001; ****P < 0.0001.

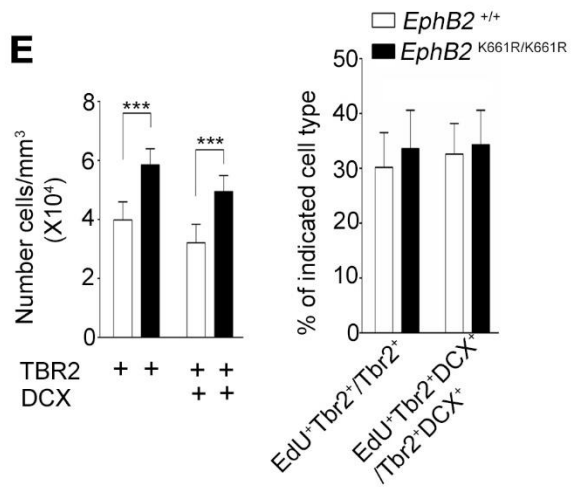
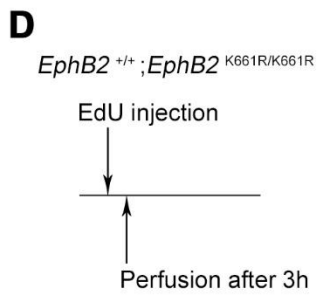
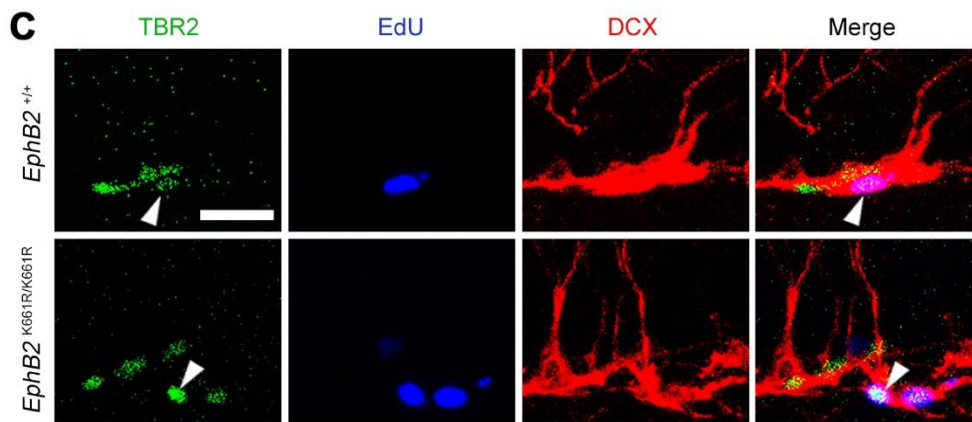
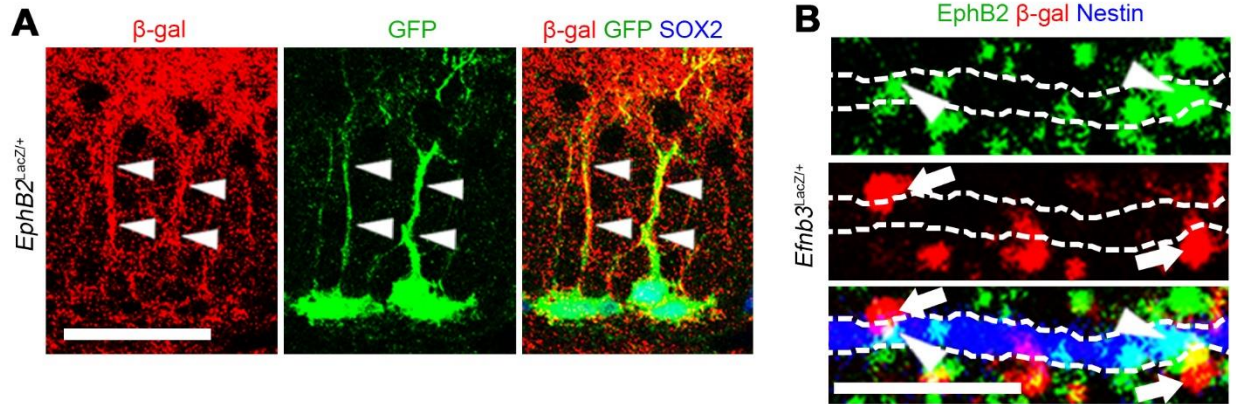


Fig. S10. EphB2 kinase-dependent signaling is required for the maintenance of quiescent rNSCs. (A) Confocal microscopy images of adult hippocampal sections of *EphB2*^{LacZ/+} show β -gal (red), Nestin-GFP (green), and SOX2 (red) triple-labeled processes (arrowheads) of NSCs projecting radially from the SGZ. Scale bar, 50 μ m. (B) Direct contact of EphB2 (green, arrowheads) on process of rNSC (blue, arrows) and ephrin-B3 (red) was detected *in vivo*. Scale bar, 2.5 μ m. (C) Composite confocal images showing EdU incorporated Tbr2 cells. Scale bar, 25 μ m. (D) Experimental paradigm for EdU injection of *EphB2*^{K661R/K661R} mice. (E) Quantitative analysis showing that *EphB2*^{K661R/K661R} mice have increased numbers of Tbr2⁺ cells, while the proliferation rate remain unchanged. n = 3 for each group. Result presented as mean \pm SEM. *P < 0.05; ***P < 0.001.

Supplementary Movies

Movie S1. Voluntary running behavior of a mouse in the running wheel. A mouse were putted in a closed running wheel that allows them to voluntarily running for 2 hours per day in a 7 day or 30 day training trials.

Movie S2. In vivo fiber photometry of Ca^{2+} signal of DG granule neurons during running trials. Adult C57 mice were injected with AAV2/9-hSyn-GCaMP6s into DG followed by optic fiber implanted at postnatal 6 weeks. After recovery for 2 weeks, the mice were put in an open running wheel. The movie shows a representative running mouse in the open wheel with a computer screen exhibiting the curve of GCaMP6s fluorescence signal.

Movie S3. 3D reconstruction of confocal images of rNSCs and GCs. The 3D reconstruction of confocal images were simulated with LAS X software in Nestin-GFP mice which had been injected with AAV-CaMKII-mCherry in DG. The rNSCs were visualized with green and the GCs were labeled with red. These data show a direct contact of rNSCs and GCs in DG area.